Surface Roughness and Knoop Indentation Micro-Hardness Behavior of Aluminium Oxide (Al_2O_3) and Polystyrene $(C_8H_8)_n$ Materials

Mohammad S. Alsoufi[1, *], Mohammed W. Alhazmi[1], Hamza A. Ghulman[1], Shadi M. Munshi[1] and Sufyan Azam[1]
[1]Department of Mechanical Engineering, College of Engineering and Islamic Architecture, Umm Al-Qura University, Makkah, KSA
[*]Corresponding author: mssoufi@uqu.edu.sa

***Abstract*-- In this paper, the surface roughness and Knoop indentation micro-hardness behavior of aluminium oxide (Al_2O_3) and polystyrene $(C_8H_8)_n$ materials were investigated. This study was conducted experimentally. Thus, the mean value of the surface roughness, R_a, for aluminium oxide (Al_2O_3) was (R_a = 0.09 µm, ±SD = 0.01), whereas for polystyrene $(C_8H_8)_n$ it was (R_a = 1.95 µm, ±SD = 0.29). Here, the surface profile has some uncoated sites and/or deep valleys as the skewness, R_{sk}, tends to be associated with a negative value for both samples. The skewness, R_{sk}, and kurtosis, R_{ku}, for aluminium oxide was -0.20 and 3.60, respectively, and for polystyrene was -1.41 and 6.45, respectively. Besides, the ratio of the two surface roughness profile (peak-to-valley) parameters R_q/R_a was about 1.22 (for aluminium oxide) and was about 1.35 (for polystyrene). Moreover, the total mean value and the total standard deviation value of the Knoop indentation micro-hardness for aluminium oxide (Al_2O_3) was (H_K = 2072.4, ±SD = 120.8) and for polystyrene $(C_8H_8)_n$ was (H_K = 18.6, ±SD = 1.38). Furthermore, the mean and standard deviation values of the elastic modulus for the aluminium oxide (Al_2O_3) material was (E = 372.95 GPa, ±SD = 9.4) with a Poisson ratio of v = 0.22, whereas, for the polystyrene $(C_8H_8)_n$ material it was (E = 3.03 GPa, ±SD = 0.1) with a Poisson ratio of v = 0.33.**

***Index Term*-- Surface Roughness, Knoop; Indentation, Micro-Hardness.**

1. INTRODUCTION

Nano-technology applications have shown extraordinary evolution in recent years. This is the result of two major issues: (1) increased availability of micro- and nano-scale engineered materials [1, 2] and (2) increased availability of micro- and nano-scale devices [3, 4]. An increased demand for micro- and nano- components have been taken into account where there is rapid growth in applications in telecommunications equipment, automotive engineering industry [5], information technology, bio-medical industry and house-used electronics products. Today, an enormous number of engineering materials are available in the industry to the engineers for design, testing and manufacturing of products for many applications. These engineering materials range from general metallic materials, for instance, cast iron, brass, copper, etc., which have remained in recent use, to the more lately industrialised advanced materials, for example, ceramics, polymers and composites. Therefore, intensive studies have been carried out to improve productivity, efficiency and indeed economic effectiveness.

In this paper, aluminium oxide (Al_2O_3) also known as alumina and polystyrene $(C_8H_8)_n$ have been investigated as they are the major engineering materials regarding surface roughness, R_a, and Knoop indentation micro-hardness, H_K. The remarkable properties of aluminium oxide (Al_2O_3) materials make them particularly well-suited to tribological applications [6]. These characteristics include the high value of hardness, a low coefficient of expansion, low reactivity, ability to operate efficiently at very high loads and temperatures, high thermal conductivity, high dielectric constant, excellent corrosion protection and wear resistance, excellent mechanical properties and chemical purity, good adhesion to glass substrate and transparency over a wide range of wavelength [7-9] and in some unique biomedical applications such as dental and medical use, cell growth control, tissue engineering and cell attachment [10]. On the other hand, polystyrene $(C_8H_8)_n$ is a thermo-plastic polymer material that has a considerable number of benefits. Among these is the fact that, it can be synthesized, processed and fully recycled and reused again. Also, it is relatively resistant to thermal degradation and it shows high values of toughness and stiffness. Its optical transparency as well makes it attractive in terms of thermal insulation and/or packaging applications [5].

2. EXPERIMENTAL PROCEDURES

2.1. Materials Studies and Methods

Two industrial engineering materials, namely aluminium oxide (Al_2O_3) and polystyrene $(C_8H_8)_n$ were investigated with identical dimensions of a length of 12 × 12 × 3 mm. Before conducting each test, both samples were ultrasonically cleaned for 15 minutes each using an ultrasonic bath (CREST Ultrasonic, CP1200D, USA) first of all in 100% pure acetone (C_3H_6O), then in isopropyl alcohol (C_3H_8O) and lastly in ethyl alcohol (C_2H_6O). After the cleaning procedure was finished, both samples were stored for at least 24 hrs. in the same environmental conditions that would be used for the investigation in order to allow the sample surface profile to equilibrate with the environmental conditions. The procedure described was judged to be adequate at this stage and is consistent with the following publication [11]. In this work, the surface roughness was performed using high precision stylus-type Taly-Surf®, whereas, micro-hardness was

conducted using Knoop micro-hardness. It should be noted that, the entire load-test series was held without lubricant on the sample surface. Besides, the entire test series took place in an artificial atmosphere, with an ambient air temperature of 20±1°C and a relative humidity of 40±5% RH. Figure 1 shows the SEM surface morphology of the aluminium oxide (Al_2O_3) and polystyrene $(C_8H_8)_n$ used for the experiments.

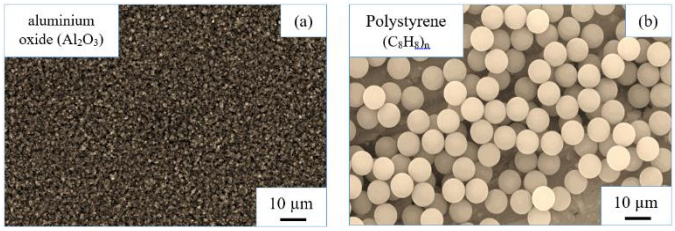

Fig. 1. SEM images of the (a) aluminium oxide (Al_2O_3) and (b) polystyrene $(C_8H_8)_n$ used for the experiments

2.2. Surface Roughness Procedure

The surface roughness profile (as shown in Figure 2) of samples was analyzed to determine the statistical parameter of average surface roughness, R_a, using high precision stylus-type Taly-Surf® (from Taylor Hobson Precision, Inc.). The device has a resolution up to 0.8 nm over a measuring range of 12.5 mm, including a data spacing of 0.125 µm. A nominal of 2 µm conisphere stylus-type was used with an average contact force of 0.7 mN and the traverse speed was maintained constant at 0.5 mm s^{-1}. The errors of surface roughness, R_a, were calculated from the standard deviation (±SD) of the absolute values of height deviation. The traces were auto-leveled set-up to a linear least-squares straight line regression and filtered with 0.80 mm cut-off. The surface parameters were selected and consistent with the recommendations in the literature review [12-17] and also with respect to the processing data facilities available. Each test condition was repeated constantly at least three times at three different locations on the surface zone in order to ensure the repeatability and reproducibility of the results. The "*new*" location was at least ±1 mm (step direction) from the prior one, as shown in Figure 3. Certainly, this method should have avoided any modification of the counter-body surface, e.g., due to tribological effect, which might occur during the test performance and affect the measurements in the following analysis (step direction). All experiments were performed with a typical arrangement of ball-on-flat. Performance of all tests was completed by using a single scan mode of 10 mm length, for more details, see [18-20]. Standard calibration performance showed that the cantilever beam system of the test-rig was a linear spring-mass system ($R^2 > 0.99$), with <1% absolute uncertainties of reading data and the measurement resolution down to at worst 50 nm, with 95% level of confidence, for more details, see [21].

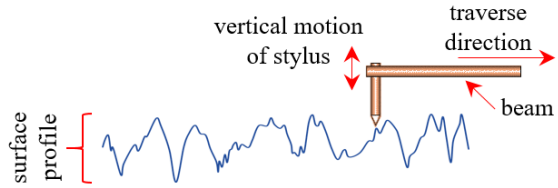

Fig. 2. Schematic illustration of stylus with 2 µm conisphere tip and surface profile

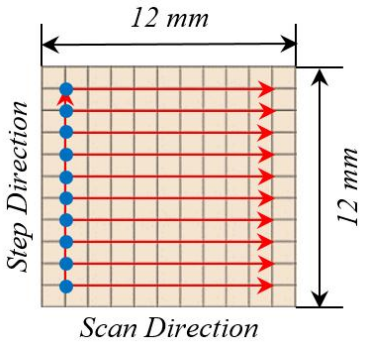

Fig. 3. Schematic diagram of the sample to be tested and the scan step direction of the stylus

2.3. Knoop Micro-Hardness Procedure

The indentation micro-hardness testing method is extensively used to designate some material parameters for a variety of research-and-development endeavors [22-25]. As an alternative to the Vicker's diamond test, mainly to asses very thin layers, Knoop micro-hardness indenter (H_K) and the shape of an impression has been used here. In 1939, The H_K and the test procedure were established at the National Bureau of Standards (now NIST) [26]. The micro-hardness of aluminium oxide (Al_2O_3) and polystyrene $(C_8H_8)_n$ samples were measured using a Knoop's diamond shape (Microhardness, Zwick Roell Indentec ZHV, Germany). Both materials were impressed with a series of standard loads and different times. Bear in mind, no cracks have been observed on the surface topography of the material, thereby providing an indentation size that allowed measurement of surface hardness of this material. Each test condition was conducted at least three times. The mean value of three readings for each trial condition was recorded as the H_K value of a specimen. The H_K test used a lozenge-based pyramid shape with the angle, θ, between the two opposite faces being 172°30' and the other two faces being 130°, as shown in Figure 4 [27]. Calculation of the H_K value considers the projected area of the contact in the plane of the material. The projected area is calculated using the length of the indent by knowing the general theory of the relationship between the width, *W*, and the length, *L*, of the impression on the sample to be tested. The Knoop indentation micro-hardness (H_K) test is conducted in the same manner, and with the same test-rig, as the Vicker's diamond test. However, only the long diagonal is measured. The Knoop indentation micro-hardness (H_K) is calculated using the following formula [28]:

$$H_K = \frac{P}{A_K} = \frac{P}{L^2 \frac{\tan\left(\frac{\emptyset}{2}\right)}{2\tan\left(\frac{\emptyset}{2}\right)}} = 14.229\frac{P}{L^2} \quad (1)$$

where, P is the applied normal load in Newton, L is the long indentation diagonal in µm and 14.229 is the geometrical constant of the diamond pyramid.

The calibration performance with test block thickness of 10.188 mm has been done using IN45259L Knoop reference hardness block at an ambient temperature of 20±1°C and a relative humidity of greater than 40±5% RH. The hardness value was calibrated on a machine complying with the requirements of BS EN ISO 4545-3:2005 having hardness scales traceable to the international weighing machine defined by PTB Germany. The mean hardness value was 476.0 H_K, the maximum value was 481.4 H_K and the minimum 472.0 H_K, with the uncertainty of 5.0 H_K and coverage factor of 2.87, providing a level of confidence of approximately 95%.

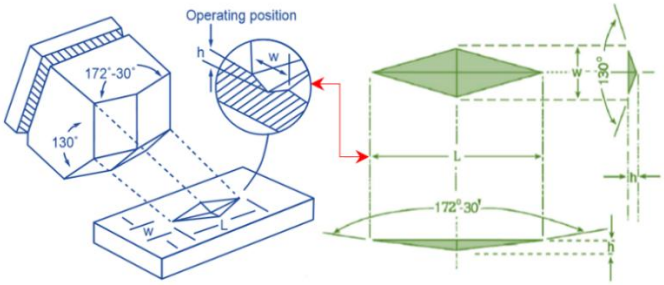

Fig. 4. Knoop indentation and diagonal indentation length, adapted from [28]

3. RESULTS AND DISCUSSIONS

3.1. Surface Roughness Data Analysis

The repeatability measurement of the surface roughness over 10 mm scan (step direction × scan direction) has been performed over aluminium oxide (Al_2O_3) and polystyrene $(C_8H_8)_n$ samples, as shown in Figure 5. As can be seen, the mean value of the surface roughness, for aluminium oxide (Al_2O_3) was (R_a = 0.09 µm, ±SD = 0.01), whereas for polystyrene $(C_8H_8)_n$ it was (R_a = 1.95 µm, ±SD = 0.29). The roughness distribution parameters of skewness, R_{sk}, and kurtosis, R_{ku}, were also calculated as shown in Table I. The skewness is a measure of the asymmetric spread of the surface height and the kurtosis represents the peakedness of the distribution. Most of the polymer films have positive skewness values and a kurtosis larger than 3, and these surfaces are generally flat but with isolated lump sites. Here, the surface profile has some deep valleys or uncoated sites as the skewness tends to be a negative value for both samples. The skewness, R_{sk}, and kurtosis, R_{ku}, for aluminium oxide were -0.20 and 3.60, respectively. On the other hand, the skewness, R_{sk}, and kurtosis, R_{ku}, for polystyrene were -1.41 and 6.45, respectively. Besides, the ratio of the two surface roughness profile parameters R_q/R_a was about 1.22 (for aluminium oxide) and about 1.35 (for polystyrene).

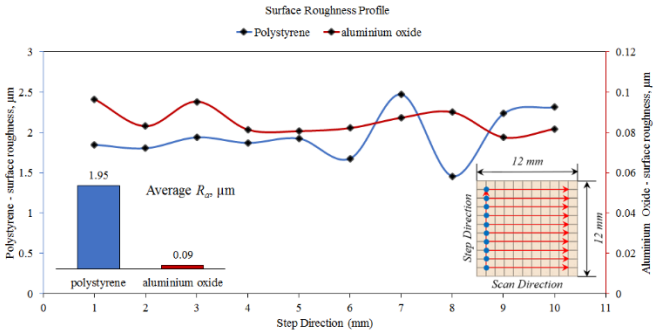

Fig. 5. Surface roughness values of aluminium oxide (Al_2O_3) and polystyrene $(C_8H_8)_n$

TABLE I
Roughness distribution parameters of polystyrene and aluminium oxide samples

Parameters	Unit	Polystyrene		Aluminium Oxide	
		Mean	±SD	Mean	±SD
R_a	µm	1.95	0.29	0.09	0.01
R_q		2.63	0.40	0.11	0.01
R_t		17.16	2.65	0.73	0.10
R_z		13.09	1.67	0.58	0.05
R_{sk}	-	-1.41	0.29	-0.20	0.33
R_{ku}	-	6.45	1.88	3.60	0.78

3.2. Knoop Micro-Hardness Data Analysis

The repeatability performance of the Knoop indentation micro-hardness, H_K, has been performed over aluminium oxide (Al_2O_3) and polystyrene $(C_8H_8)_n$ samples, as shown in Figures 6 and 7, respectively. For aluminium oxide performance, the sample was impressed with a load range of 200, 300, 500 and 1000g with the holding time after completion of the indentation being 20, 25, 30 and 35 seconds for each load. Figure 6 shows the individual mean and standard deviation values of aluminium oxide (Al_2O_3) for each load with holding period. As can be seen, the total mean value and the total standard deviation value of the Knoop indentation micro-hardness for aluminium oxide (Al_2O_3) was (H_K = 2072.4, ±SD = 120.8). There is no marked variation in Knoop indentation micro-hardness results of aluminium oxide (Al_2O_3) as regards the holding time and loads, except the 500 g with a holding time of 35 second showing the slightly higher value of H_K. On the other hand, for polystyrene $(C_8H_8)_n$ performance, the sample was impressed with a load range of 10, 25, 50, 100 and 200 g with the holding time after completion of the indentation being 15, 20, 25 and 30 seconds for each load. Figure 7 shows the individual mean and standard deviation values of polystyrene $(C_8H_8)_n$ for each load with holding time period. As can be seen, the total mean value and the total standard deviation value of the Knoop indentation micro-hardness for polystyrene $(C_8H_8)_n$ was (H_K = 18.6, ±SD = 1.38). Again, there is a slight variation in Knoop indentation micro-hardness results of polystyrene $(C_8H_8)_n$ with the holding time and loads, except for the 200g with all series of holding times showing approximately the same value of H_K. Figure 8 shows some random surface topography images of the Knoop indentation micro-hardness test for both methods at 1000g and 35 seconds for aluminium oxide (Al_2O_3) and at 200g and 30 seconds for polystyrene $(C_8H_8)_n$. Also, Figure 9

shows the variation of the Knoop indentation micro-hardness test for aluminium oxide (Al_2O_3) with different loads including a stable polynomial regression relationship of $R^2 > 0.9237$. The holding time under various peak loads after completion of the indentation was 25 seconds. Figure 10 shows the variation of the Knoop indentation micro-hardness test for polystyrene $(C_8H_8)_n$ with different loads including a stable polynomial regression relationship of $R^2 > 0.9821$. The holding time under various peak loads after completion of the indentation was 20 seconds. These were marked difference results, as expected, for both samples, including the high value of hardness in aluminium oxide (Al_2O_3), which is more related to the chemical, mechanical and physical properties of the material. Thus, the aluminium oxide (Al_2O_3) results make it extremely attractive to micro- and nano-tribology applications. In contrast, the polystyrene $(C_8H_8)_n$ sample shows a very low value with respect to hardness, which makes it an extremely attractive material for thermal insulation, packaging and automotive applications.

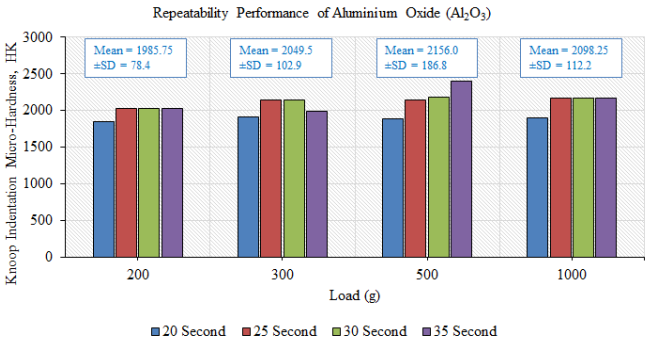

Fig. 6. Knoop indentation micro-hardness values of aluminium oxide (Al_2O_3)

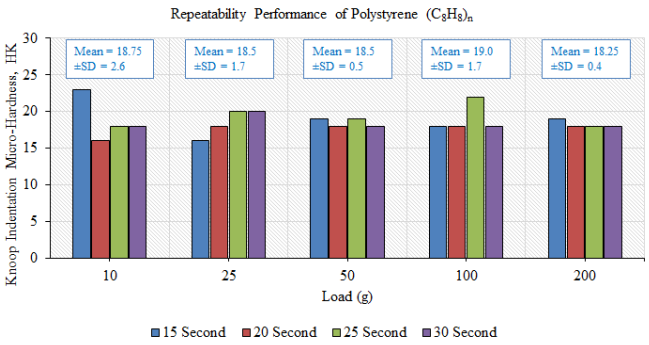

Fig. 7. Knoop indentation micro-hardness values of polystyrene $(C_8H_8)_n$

Apparently, H_K is a function of applied small indentation test loads as shown in Figures 9 and 10, where there is no constant value for the micro-hardness (load-dependent hardness region). Weight variation of this type has been observed in several studies [24, 29, 30]. This behavior is called reverse indentation size effect (RISE), in which plastic deformation is predominant [29]. At high indentation test loads, P_{max}, the H_K value is approximately constant with respect to the load and a single, well-defined micro-hardness value exists (load-independent hardness region). In the literature review, the load-independent hardness area has been referred to as "*true/real*" micro-hardness and this behavior is also named indentation size effect (ISE) and typically involves a decrease in the apparent micro-hardness with increasing load, i.e., with increasing the size of the indentation [23, 28, 29, 31-33].

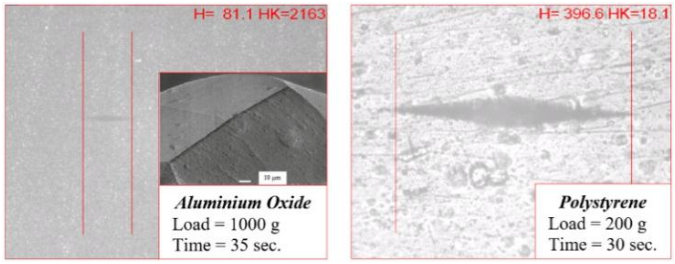

Fig. 8. Surface topography image of the H_K test for aluminium oxide and polystyrene, showing good tip definition, with SEM image of the tip of Knoop

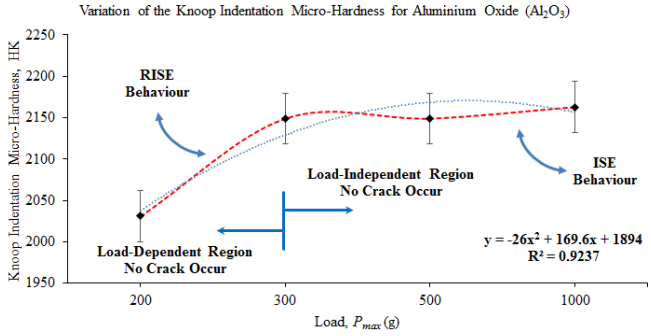

Fig. 9. Variation of the H_K test for aluminium oxide (Al_2O_3) with different loads. The net holding time after completion of the indentation was 25 second

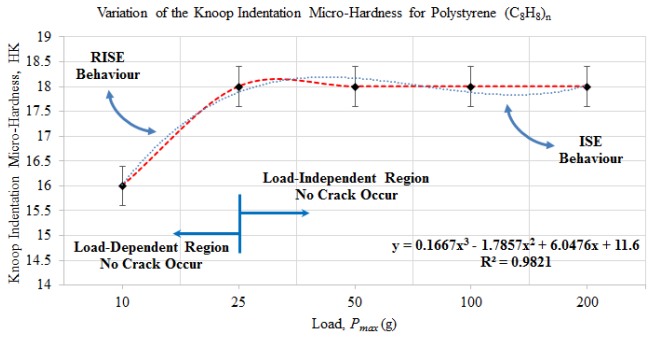

Fig. 10. Variation of the H_K test for polystyrene $(C_8H_8)_n$ with different loads. The net holding time after completion of the indentation was 20 second

The primary goal of nano-indentation testing is to obtain the elastic modulus, E, and hardness value of the material from experimental data of the load and depth-sensing indentation of penetration. In a typical assessment, the load and depth-sensing of penetration are recorded as load, P, is applied from zero (no load) to a maximum value (load) and then from maximum value (load) backwards to zero (no load). Figure 11 shows the two load/displacement curves of an average of 10 different measurements for indentations in aluminium oxide and polystyrene with a schematic drawing of the loading/unloading data process showing the contact geometry parameters. These measured parameters including the maximum load, P_{max}, the depth below the specimen's free surface, h_{max}, the contact circle depth, h_c, the elastic unloading

slope, *dP/dh* allow sample modulus and hardness to be calculated, the residual impression depth, h_r, and the displacement associated with the elastic recovery during unloading, h_e, and the final depth, h_f.

The average value of the micro-hardness for aluminium oxide (Al_2O_3) is around 2098.25 H_K and for polystyrene $(C_8H_8)_n$ is around 18.6 H_K. The indentation depth for aluminium oxide (Al_2O_3) is around 2500 nm at 700 mN load, while the indentation depth for polystyrene $(C_8H_8)_n$ is around 2500 nm at 300 mN load, indicating a near surface effect on mechanical properties. From the curve load/displacement, it can see that the elastoplastic deformation appears in polystyrene sample cases more than is the case with the aluminium oxide sample. Thus, the polystyrene sample is more resistant to contact loading than is the aluminium oxide (Al_2O_3) sample. Also, the loading area represents the plastic deformation while the unloading area represents the elastic recovery.

The Oliver and Pharr analysis procedure [34] begins with the fitting an unloading curve (backwards) to an empirical data power-law relationship, as stated in Equation (2):

$$P = \alpha\left(h - h_f\right)^m \tag{2}$$

where, P, is the indentation test load, h, is the penetration depth, h_f, is the final unloading depth, α, is a geometric constant and m is a power-law fitting constant that are related to the geometry of the indenter. Typically, m, values are varying from 1.0 to 2.0 depending on the indenter geometry. The unloading contact stiffness, S, is established by differentiating Equation (3) at the maximum depth of penetration, $h = h_{max}$:

$$S = \left(\frac{dP}{dh}\right)_{h=h_{max}} = \alpha m\left(h_{max} - h_f\right)^{m-1} \tag{3}$$

The contact depth, h_c, along which contact is made between the indenter and the specimen, $h_c = h_{max} - h_s$, is calculated using the following Equation (4):

$$h_c = h_{max} - \beta\frac{P_{max}}{S} \tag{4}$$

where, P_{max}, is the peak indentation test load and β is the dimensionless parameter ($\beta \approx 0.72$ for a hard conical punch, 0.75 for a paraboloid surface of revolution and 1.00 for a flat face punch) [34-37]. On the other hand, the peak indentation test load-penetration depth behavior can be usefully used in defining a reduced elastic modulus. The effective elastic modulus E_{eff} can be calculated from the initial slope of the unloading curve, as stated in Equation (5):

$$E_{eff} = \frac{1}{2\beta\left(\frac{\pi}{A}\right)^{1/2}}S \tag{5}$$

Equation (5) applies to a good number of axisymmetric intender geometries. Finally, the elastic modulus, E, of the material can be obtained from Equation (6):

$$\frac{1}{E_{eff}} = \frac{(1-v^2)}{E} + \frac{(1-v_i^2)}{E_i} \tag{6}$$

where, v, is the Poisson's ratio of the material and v_i and E_i correspond to the elastic properties of the indenter. In the case of polymer materials, because $E_i >> E$, Equation (6) can be directly given as stated in Equation (7):

$$E = E_{eff}(1-v^2) \tag{7}$$

Figures 12 and 13 show the variation of the elastic modulus, E, test for aluminium oxide (Al_2O_3) and polystyrene $(C_8H_8)_n$ with different loads including a stable polynomial regression relationship of $R^2 > 0.9235$ and $R^2 > 0.9821$, respectively. After completion, the remaining holding time of the indentation was 25 seconds. Both graphs (for elastic modulus) follow the same pattern as shown in figures (for micro-hardness). The values of mean and standard deviation (±SD) of the elastic modulus, E, for the aluminium oxide (Al_2O_3) material was E = 372.95 ± 9.4 GPa with a Poisson's ratio of v = 0.22. Whereas, for the polystyrene $(C_8H_8)_n$ material it was E = 3.03 ± 0.1 GPa with a Poisson's ratio of v = 0.33.

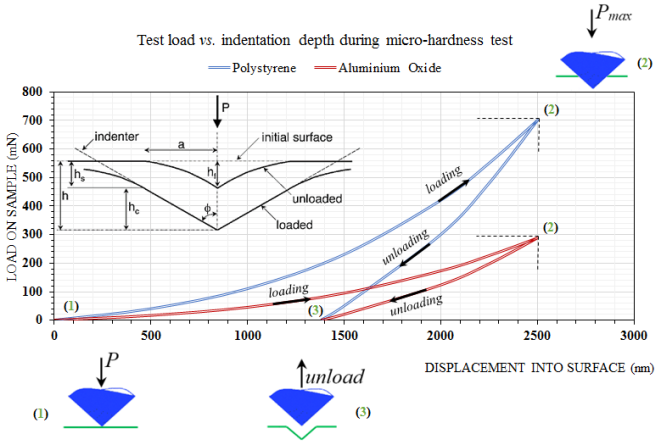

Fig. 11. Load-displacement curves for indentations in polystyrene and aluminium oxide with schematic illustration of the loading/unloading process showing parameters characterizing the contact geometry

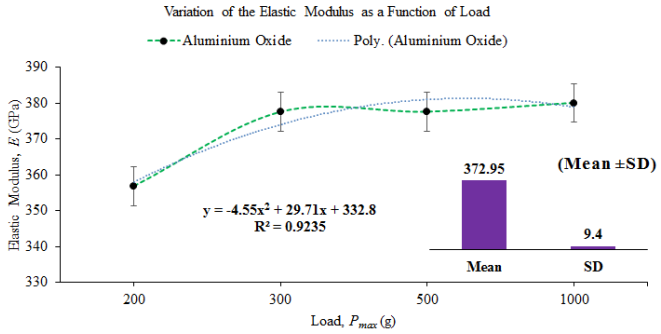

Fig. 12. Variation of the elastic modulus test for aluminium oxide (Al_2O_3) with different loads. The net holding time after completion of the indentation was 25 second

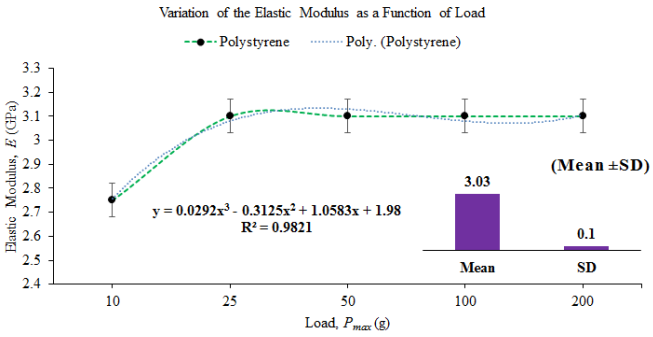

Fig. 13. Variation of the elastic modulus test for polystyrene $(C_8H_8)_n$ with different loads. The net holding time after completion of the indentation was 20 seconds

4. SUMMARY AND CONCLUSIONS

In the present work, the surface roughness parameters and Knoop indentation micro-hardness H_K were used to evaluate the surface layer of aluminium oxide and polystyrene samples. Also, the intention was to set up a correlation between the two mechanical method procedures used here. In the present study, the overview of some remarkable results observed from the investigation carried out are as follows:

- The mean and standard deviation values of the surface roughness profile, R_a, for aluminium oxide (Al_2O_3) was (R_a = 0.09 µm, ±SD = 0.01), whereas for polystyrene $(C_8H_8)_n$ it was (R_a = 1.95 µm, ±SD = 0.29).
- The skewness, R_{sk}, and kurtosis, R_{ku}, for aluminium oxide were -0.20 and 3.60, respectively. On the other hand, the skewness, R_{sk}, and kurtosis, R_{ku}, for polystyrene were -1.41 and 6.45, respectively.
- The ratio of the two surface roughness profile parameters R_q/R_a was about 1.22 (for aluminium oxide) and about 1.35 (for polystyrene).
- The measured H_K values were obviously load-dependent at 300g for aluminium oxide (Al_2O_3) and at 25g for polystyrene $(C_8H_8)_n$ samples.
- The variation of H_K follows the reverse ISE trend, i.e., an increase in H_K on load in the low-load region beyond where it becomes relatively constant.
- The total mean value and the total standard deviation (±SD) value of the H_K for aluminium oxide (Al_2O_3) were (H_K = 2072.4, ±SD = 120.8) and for polystyrene $(C_8H_8)_n$ was (H_K = 18.6 µm, ±SD = 1.38).
- The mean and standard deviation (±SD) values of the elastic modulus, E, for the aluminium oxide (Al_2O_3) material was E = 372.95 GPa, ±SD = 9.4 with a Poisson's ratio of ν = 0.22. Whereas, for the polystyrene $(C_8H_8)_n$ material was E = 3.03 GPa, ±SD = 0.1 with a Poisson's ratio of ν = 0.33.

REFERENCES

[1] Aly, A., M. Mahmoud, and A. Omar, *Enhancement in Mechanical Properties of Polystyrene Filled with Carbon Nano-Particulates (CNPS).* World Journal of Nano Science and Engineering, 2012. **2**(2): p. 103-109.

[2] Nasir, A. and A. Kausar, *A Review on Materials Derived from Polystyrene and Different Types of Nanoparticles.* Polymer-Plastics Technology and Engineering, 2015. **54**(17): p. 1819-1849.

[3] Alsoufi, M. S., *A high dynamic response micro-tribometer measuring-head*, in School of Engineering. 2011, University of Warwick: Coventry.

[4] Chetwynd, D. G. and M. S. Alsoufi. *A novel micro-friction measuring-head using force-feedback compensation*. in *Proc. SPIE 7544, Sixth International Symposium on Precision Engineering Measurements and Instrumentation*. 2010. Hangzhou, China.

[5] Baltá-Calleja, F. J., Cagiao, M. E., Adhikari, R. and Michler, G. H. *Relating microhardness to morphology in styrene/butadiene block copolymer/polystyrene blends.* Polymer, 2004. **45**(1): p. 247-254.

[6] Takadoum, J., *Materials and Surface Engineering in Tribology*. 1st ed. 2008, USA: John Wiley & Sons. 242.

[7] Zhao, Z. W., Tay, B. K., Yu, G. Q., Chua, D. H. C., Lau, S. P. and Cheah, L. K. *Optical properties of aluminium oxide thin films prepared at room temperature by off-plane filtered cathodic vacuum arc system.* Thin Solid Films, 2004. **447**–**448**: p. 14-19.

[8] Aguilar-Frutis, M., Garcia, M., Falcony, C., Plesch, G. and Jimenez-Sandoval, S. *A study of the dielectric characteristics of aluminum oxide thin films deposited by spray pyrolysis from Al(acac)3.* Thin Solid Films, 2001. **389**(1–2): p. 200-206.

[9] Koski, K., J. Hölsä, and P. Juliet, *Properties of aluminium oxide thin films deposited by reactive magnetron sputtering.* Thin Solid Films, 1999. **339**(1–2): p. 240-248.

[10] Teare, D. O. H., N. Emmison, C. Ton-That and R. H. Bradley *Cellular Attachment to Ultraviolet Ozone Modified Polystyrene Surfaces.* Langmuir, 2000. **16**: p. 2818-2824

[11] Alsoufi, M. S., *Dry Micro-frictional Properties of Ceramic and Polystyrene Oscillating Against a Sapphire Counterbody at Small-Scale Loads.* Engineering and Technology, 2016. **3**(5): p. 100-105.

[12] Dong, W. P., P. J. Sullivan, and K. J. Stout, *Comprehensive study of parameters for characterizing three-dimensional surface topography I: Some inherent properties of parameter variation.* Wear, 1992. **159**(2): p. 161-171.

[13] Dong, W. P., P. J. Sullivan, and K. J. Stout, *Comprehensive study of parameters for characterizing three-dimensional surface topography II: Statistical properties of parameter variation.* Wear, 1993. **167**(1): p. 9-21.

[14] Dong, W. P., P. J. Sullivan, and K. J. Stout, *Comprehensive study of parameters for characterising three- dimensional surface topography: III: Parameters for characterising amplitude and some functional properties.* Wear, 1994. **178**(1–2): p. 29-43.

[15] Dong, W. P., P. J. Sullivan, and K. J. Stout, *Comprehensive study of parameters for characterising three-dimensional surface topography: IV: Parameters for characterising spatial and hybrid properties.* Wear, 1994. **178**(1–2): p. 45-60.

[16] Alsoufi, M. S. and T. M. Bawazeer, *The Effect of Aggressive Biological Materials on a Painted Automotive Body Surface Roughness.* American Journal of Nano Research and Applications, 2015. **3**(2): p. 17-26.

[17] Bawazeer, T. M., Alsoufi, M. S., Katowah, D. and Alharbi, W. S., *Effect of Aqueous Extracts of Salvadora Persica "Miswak" on the Acid Eroded Enamel Surface at Nano-Mechanical Scale*. Materials Sciences and Applications, 2016. **7**(11): p. 754-771.

[18] Mohammad S. Alsoufi, Dhia K. Suker, Abdulaziz S. Alsabban and Sufyan Azam. *Experimental Study of Surface Roughness and Micro-Hardness Obtained by Cutting Carbon Steel with Abrasive WaterJet and Laser Beam Technologies.* American Journal of Mechanical Engineering, 2016. **4**(5): p. 173-181.

[19] Suker, D. K., M. S. Alsoufi, M. M. Alhusaini and S. A. Azam *Studying the Effect of Cutting Conditions in Turning Process on Surface Roughness for Different Materials.* World Journal of Research and Review (WJRR) 2016 **2**(4): p. 16-21.

[20] Alsoufi, M. S. and T. M. Bawazeer, *Quantifying assessment of touch-feel perception: an investigation using stylus base equipment and self-touch (human fingertip).* Umm Al-Qura University: Journal of Engineering & Architecture, 2015. **1**(1): p. 1-16.

[21] Alsoufi, M. S., *Tactile Perception of Passenger Vehicle Interior Polymer Surfaces: An Investigation using Fingertip Blind Observations and Friction Properties.* International Journal of Science and Research (IJSR), 2016. **5**(5): p. 1447-1454.
[22] Sangwal, K., B. Surowska, and P. Błaziak, *Relationship between indentation size effect and material properties in the microhardness measurement of some cobalt-based alloys.* Materials Chemistry and Physics, 2003. **80**(2): p. 428-437.
[23] Sahin, O., O. Uzun, U. Kolemen, B. Duzgun and N. Ucar *Indentation Size Effect and Microhardness Study of β-Sn Single Crystals.* Chinese Physics Letters, 2005. **22**(12): p. 3137.
[24] Gong Jianghong, Miao Hezhuo, Zhao Zhe and Guan Zhenduo. *Load-dependence of the measured hardness of Ti(C,N)-based cermets.* Materials Science and Engineering: A, 2001. **303**(1–2): p. 179-186.
[25] Sahin, O. and A. R, *Production and Mechanical Behaviour of Biomedical CoCrMo Alloy.* Chinese Physics Letters, 2011. **28**(12): p. 126201.
[26] Milan, Y., *Micro and Macro Hardness Measurements, Correlations, and Contact Models*, in *44th AIAA Aerospace Sciences Meeting and Exhibit*. 2006, American Institute of Aeronautics and Astronautics.
[27] Sanosh, K. P., Balakrishnan, A., Francis, L. and Kim, T. N. *Vickers and Knoop Micro-hardness Behavior of Coarse-and Ultrafine-grained Titanium.* Journal of Materials Science & Technology, 2010. **26**(10): p. 904-907.
[28] Güder, H. S., E. Şahin, O. Şahin, H. Göçmez, C. Duran and H. Ali Çetinkara. *Vickers and Knoop Indentation Microhardness Study of β-SiAlON Ceramic* Acta Physica Polonica A, 2011. **120**(6): p. 1026-1033.
[29] Sangwal, K., *On the reverse indentation size effect and microhardness measurement of solids.* Materials Chemistry and Physics, 2000. **63**(2): p. 145-152.
[30] Gong, J. and Z. Guan, *Load dependence of low-load Knoop hardness in ceramics: a modified PSR model.* Materials Letters, 2001. **47**(3): p. 140-144.
[31] Petrík, J. and P. Palfy, *Variability of Indentation Size Effect (ISE) of Standard Reference Block.* MAPAN, 2014. **29**(1): p. 43-50.
[32] Sahin Osman, Uzun Orhan, Sopicka-Lizer Małgorzata, Gocmez Hasan and Kölemen, Uğur. *Dynamic hardness and elastic modulus calculation of porous SiAlON ceramics using depth-sensing indentation technique.* Journal of the European Ceramic Society, 2008. **28**(6): p. 1235-1242.
[33] Osman, S., *Indentation Load Effect on Young's Modulus and Hardness of Porous Sialon Ceramic by Depth Sensing Indentation Tests.* Chinese Physics Letters, 2007. **24**(11): p. 3206.
[34] Oliver, W. C. and G. M. Pharr, *An improved technique for determining hardness and elastic modulus using load and displacement sensing indentation experiments.* Journal of Materials Research, 1992. **7**(6): p. 1564-1583.
[35] Flores, A., F. Ania, and F. J. Baltá-Calleja, *From the glassy state to ordered polymer structures: A microhardness study*. Polymer, 2009. **50**(3): p. 729-746.
[36] Oliver, W. C. and G. M. Pharr, *Measurement of hardness and elastic modulus by instrumented indentation: Advances in understanding and refinements to methodology*. Journal of Materials Research, 2004. **19**(1): p. 3-20.
[37] Sneddon, I. N., *The relation between load and penetration in the axisymmetric boussinesq problem for a punch of arbitrary profile.* International Journal of Engineering Science, 1965. **3**(1): p. 47-57.